Video Article

Ethanol-Induced Cervical Sympathetic Ganglion Block Applications for Promoting Canine Inferior Alveolar Nerve Regeneration Using an Artificial Nerve

Yoshiki Shionoya[1], Katsuhisa Sunada[2], Gentarou Tsujimoto[2], Keiji Shigeno[3], Tatsuo Nakamura[3]

[1]Department of Dental Anesthesia, Nippon Dental University Hospital at Tokyo

[2]Department of Dental Anesthesiology, Nippon Dental University School of Life Dentistry at Tokyo

[3]Department of Bioartificial Organs, Institute for Frontier Medical Science, Kyoto University

Correspondence to: Yoshiki Shionoya at ysk.shionoya@gmail.com

URL: https://www.jove.com/video/58039
DOI: doi:10.3791/58039

Keywords: Neuroscience, Issue 141, neuroscience, *in situ* tissue engineering, artificial nerve conduit, polyglycolic acid-collagen tube, cervical sympathetic ganglion block, canine model

Date Published: 11/30/2018

Citation: Shionoya, Y., Sunada, K., Tsujimoto, G., Shigeno, K., Nakamura, T. Ethanol-Induced Cervical Sympathetic Ganglion Block Applications for Promoting Canine Inferior Alveolar Nerve Regeneration Using an Artificial Nerve. *J. Vis. Exp.* (141), e58039, doi:10.3791/58039 (2018).

Abstract

Polyglycolic acid collagen (PGA-C) tubes are bio-absorbable nerve tubes filled with collagen of multi-chamber structure, which consist of thin collagen films. Favorable clinical outcomes have been achieved when using these tubes for the treatment of damaged inferior alveolar nerve (IAN). A critical factor for the successful nerve regeneration using PGA-C tubes is blood supply to the surrounding tissue. Cervical sympathetic ganglion block (CSGB) creates a sympathetic blockade in the head and neck region thus increasing blood flow in the area. To ensure an adequate effect, the blockade must be administered with local anesthetics one to two times a day for several consecutive weeks; this poses a challenge when creating animal models for investigating this technique. To address this limitation, we developed an ethanol-induced CSGB in a canine model of long-term increase in blood flow in the orofacial region. We examined whether IAN regeneration via PGA-C tube implantation can be enhanced by this model. Fourteen Beagles were each implanted with a PGA-C tube across a 10-mm gap in the left IAN. The IAN is located within the mandibular canal surrounded by bone, therefore we chose piezoelectric surgery, consisting of ultrasonic waves, for bone processing, in order to minimize the risk of nerve and vessel injury. A good surgical outcome was obtained with this approach. A week after surgery, seven of these dogs were subjected to left CSGB by injection of ethanol. Ethanol-induced CSGB resulted in improved nerve regeneration, suggesting that the increased blood flow effectively promotes nerve regeneration in IAN defects. This canine model can contribute to further research on the long-term effects of CSGB.

Video Link

The video component of this article can be found at https://www.jove.com/video/58039/

Introduction

In many cases, traumatic injury of the inferior alveolar nerve (IAN) is iatrogenic, being frequently caused by the extraction of the third molar or the placement of dental implants[1,2,3]. Injury of the IAN can lead to deficits in thermal and touch sensations as well as paresthesia, dysesthesia, hypoesthesia, and allodynia. Nerve injury is treated not only by conservative therapy but also by other methods, including suturing and autograft placement. However, these methods have drawbacks, which often include the lack of symptom improvement and neurological defects at the donor site[4,5,6].

The artificial nerve — polyglycolic acid-collagen (PGA-C) tube was originally developed in Japan. It is a bio-absorbable tube with its inner lumen filled with a spongiform collagen[7]. In animal experiments, this tube was used to enhance nerve regeneration in beagle dogs with peroneal nerve defect, and was shown to promote higher level of recovery than autologous nerve transplantation[8]. The clinical application of the PGA-C tube began in 2002 in patients with peripheral nerve injuries. Moreover, favorable clinical outcomes have been achieved in the treatment of trigeminal neuropathy (IAN and lingual nerve)[9,10,11]. A critical factor for successful nerve regeneration using PGA-C tubes is blood supply to the surrounding tissue[8]. Cervical sympathetic ganglion block (CSGB) creates a sympathetic blockade in the head and neck region and increases blood flow to the respective innervated area[12]; thus, it has been used in the treatment of complex regional pain syndrome and circulatory insufficiency[13,14,15]. However, there have been only a few experimental investigations on the efficacy of CSGB in increasing blood flow[16,17]. To ensure adequate CSGB efficiency, the blockade must be applied together with local anesthetics once or twice daily for several weeks, thus posing a challenge when generating animal models to investigate this technique. To address this limitation, in a previous study, we developed a canine model of long-term increased blood flow in the orofacial region[18]. The model was generated by performing a CSGB by injecting 99.5% ethanol. We evaluated the oral mucosal blood flow and nasal skin temperature by laser Doppler flowmetry and infrared thermography once per week for 12 weeks. We found that the blood flow of the orofacial region was increased for 7 – 10 weeks in this model.

In the present study, we evaluated the effects of ethanol-induced CSGB on nerve regeneration.

The PGA-C tube was implanted into beagle dogs across a 10-mm gap in the left IAN. A week later, CSGB was performed by injecting ethanol. Three months after surgery, we performed a variety of electrophysiological, histological, and morphological studies to evaluate the effects of CSGB on nerve regeneration. We provide a detailed protocol for IAN reconstruction using a PGA-C tube and ethanol-induced CSGB.

Protocol

This study was conducted in accordance with the Guiding Principles for the Care and Use of Animals and approved by the Committee for Animal Research of Kyoto University (Kyoto, Japan; authorization number: R-16-16). All efforts were made to minimize animal suffering, and all sections of this report adhere to the ARRIVE (Animal Research: Reporting of *in Vivo* Experiments) guidelines.

1. Fabrication of the PGA-C tube

1. To fabricate the artificial nerve conduit by means of an absorbable polyglycolic acid (PGA) tube, use a tubular braiding machine equipped with 48 spindles and five PGA fibers, comprised of bundles of 26 filaments (**Figure 1**)[18].
2. To render the PGA tube surface hydrophilic, expose it to plasma discharge.
3. Use 1% v/w atelocollagen in hydrochloride solution[7].
   NOTE: Atelocollagen is extracted from porcine skin via enzyme treatment and subjected to a virus check. It mainly consists of type I (70–80%) and type III collagen, the ratio of which is described in detail elsewhere[7]. Prepare the collagen solution by dissolving 1 g collagen in 100 mL hydrochloride solution (pH = 3.0). Since the density of the hydrochloride solution is approximately 1.0, the w/w collagen concentration is almost 1%.
4. Coat the tube with the collagen layers by repeatedly dipping it into the 1% collagen hydrochloride solution for 5 s each time.
   1. After dipping, dry the tube on a clean bench at room temperature. Perform next dipping after ensuring the tube is completely dry (about 6 h for air-drying).
   2. Repeat the coating process 10 times.
5. Subject the PGA-C tube to 140 °C for 24 h under vacuum (dehydrothermal treatment), in order to control bio-absorption and crosslinking of the collagen molecules. Perform the entire process under aseptic conditions.
   NOTE: This procedure generates a tube of 14-mm final length, 3-mm inner diameter, and 50-μm wall thickness.

2. Surgical Procedure Set-up

1. Use adult male beagles weighing 9.0 to 13.0 kg.
   1. House animals in separate cages, under controlled kennel conditions (12-h light and dark cycle).
   2. Provide solid food and water *ad libitum*.
2. Weigh the beagles.
3. Autoclave all surgical instruments.
4. Don sterilized gloves and disinfect all surfaces of the operating setting with an 80% ethanol solution. Discard the used gloves.
5. Perform surgical handwashing.
6. Put on a fresh mask, gown, and sterile gloves.

3. Anesthesia and Skin Preparation

1. Anesthetize the dog with a mixture of 5 mg/kg ketamine hydrochloride and 1 mg/kg xylazine by an intramuscular injection.
2. Intubate by a tracheal tube of 7.5 mm diameter and 25 cm length.
3. Place the dog on the right lateral position. Maintain general anesthesia with 3.2% sevoflurane with oxygen (1.0 L/min).
4. Use a heating pad to maintain body temperature at 37 °C.
5. Apply an ophthalmic gel over the anterior surface of the eyes to avoid corneal abrasion.
6. Carefully shave the surgical field (left side chest area) using surgical clippers. Spray a substantial amount of alcoholic solution over the operative site. Wait at least 15 sec. Repeat the application 3 times.
7. Record the heart rate and oxygen saturation during surgery.

4. Inferior Alveolar Nerve Reconstruction Using PGA-C tube: Development of the Reconstruction-only Model

1. Inject 3 mL of 1% lidocaine using a 27 G needle to the left mandibular gingiva as a local anesthetic and analgesic.
2. Perform a 5-cm transverse incision with a number 15 scalpel blade in the left mandibular gingiva, to expose the mandibles of the animal.
3. Use piezoelectric ultrasonic vibrations to grind the proximal aspect of the mandible into a 3-cm × 8-mm rectangle through the posterior mental foramen.
   NOTE: The vibration frequency was 28 – 32 kHz.
4. Remove the frontal part of the mandibular bone plate (dimensions, 3 cm × 8 mm) to expose the left IAN (**Figure 2A**)[18].
   NOTE: The reconstruction site corresponds to the root apex of the first molar
5. Transect the IAN with a scalpel to remove a 10-mm segment.
6. Insert the proximal and distal stumps of the severed nerve into the nerve tube to a depth of 2 mm.
7. Use 8-0 nylon sutures and a surgical microscope at 8X magnification to suture the tube to the proximal and distal nerve ends (**Figure 2B**)[18].
8. Return the bone plate to its original site in the mandible.

9. Close the wound with 4-0 nylon sutures.
10. One day after surgery, confirm that the mandibular bone plate is in its proper position.
    1. 4.10.1 Perform computed tomography (CT) imaging of the facial bone under anesthesia. Set CT parameters as follows: 120 kVp, 200 mAs, 0.5 mm/s, 0.5-mm slice thickness.
        1. Administer anesthesia using a mixture of 5 mg/kg ketamine hydrochloride and 1 mg/kg xylazine (**Figure 3**).
11. Administer ampicillin (100 mg/day) as an antibiotic and acetaminophen (100 mg/day) as an analgesic for a week after surgery.

5. Ethanol-induced CSGB: Development of the Reconstruction + CSGB Model

1. Perform IAN reconstruction as described in section 4 and allow a week for recovery.
2. Anesthetize the animal with 1.5% sevoflurane in oxygen (4 L/min) and air (6 L/min). Shave and clean the intended surgical field, as described in section 3.
3. Mark the incision line with a surgical skin marker by drawing a line on the left side chest area (**Figure 4**, the incision line is 20 cm in length).
4. Inject 5 mL of 1% lidocaine using a 21 G needle to the left side chest area as a local anesthetic and analgesic.
5. Incise the left side chest skin with a number 10 scalpel blade.
6. Incise the fat layer with an electric scalpel to expose the muscle fascia.
7. Expose the serratus ventralis muscle and scalenus muscle.
8. Raise the serratus ventralis muscle and scalenus muscle from ventral to dorsal to expose the second and third ribs (**Figure 5**).
9. Perform a left lateral thoracotomy at the second and third intercostal space to expose the left cervical sympathetic ganglion (**Figure 6**).
10. Inject 0.2 mL of 99.5% ethanol into the cervical sympathetic ganglion using a 30 G needle under direct visualization (**Figure 7**).
11. Close the intercostal space with interrupted 1-0 absorbable stitches.
12. Close the skin with interrupted 3-0 nylon stitches.
13. Administer ampicillin (100 mg/day) as an antibiotic and acetaminophen (100 mg/day) as an analgesic for a week after surgery.
14. At 1 week after CSGB, measure facial skin temperature with infrared thermography to confirm the CSGB.

6. Electrophysiological Recordings

1. To measure sensory nerve action potential (SNAP) and sensory nerve conduction velocity (SCV) of the IAN three months after reconstruction, anesthetize animals as described in section 3.
   NOTE: SNAP and SCV should be measured on both the experimental and normal control sides for each dog in both treatment groups.
2. Make an incision in the left mandibular gingiva with a number 10 scalpel blade.
3. Carefully remove the mandibular bone plate to avoid physically damaging the regenerated nerve.
4. Stimulate the IAN using a pair of needle electrodes, to record the SNAP and SCV.
    1. Insert the electrodes proximally to the nerve conduit.
    2. Apply 10-kHz electrical stimulus 20 times.
5. Analyze the results.
    1. Determine SNAP by calculating the average response amplitude to the electrical stimulation.
    2. Measure the peak latency and peak amplitude from the chart recordings.
    3. Calculate the recovery index with the following equation: peak amplitude of the left IAN of the reconstruction-only or reconstruction + CSGB group / peak amplitude of the normal control (central segment of the right IAN in the reconstruction-only group)[19,20].

7. Histological Analysis

1. **Section Preparation**
    1. Three months after reconstruction, harvest the left IAN, including 1 cm of the nerve on either side of the reconstructed site.
    2. Harvest the right IAN at the level corresponding to the harvest site on the left side.
    3. Prefix the harvested nerves by immersion in 2.5% glutaraldehyde in a 0.1 M cacodylate buffer solution (pH 7.4, 48 °C, 24 h).
    4. Postfix with 2% osmium tetroxide solution (48 °C, 4 h) and potassium ferrocyanide in 0.1 M phosphate buffer solution (pH 7.4, 2 h).
    5. Dehydrate the nerves with a series of graded ethanol solutions.
    6. Embed in epoxy resin (paraffin).
    7. Section the specimens at a thickness of 0.5 – 1.0 µm.
2. **Toluidine Blue Staining and Morphological Analysis**
    1. Stain sections with toluidine blue solution.
    2. Obtain microscopy images using an optical microscope, at 400X magnification at the following regions along the samples: left IAN, the center of the regenerated segment and 2 mm distally to the stump; right IAN, the center of the IAN segment corresponding to the harvest site on the left side.
    3. Select images of all regions with regenerated nerve fibers.
        1. Randomly select 8 – 10 areas of 100 µm × 100 µm containing regenerated nerve fibers.
        2. Perform morphological analysis using an appropriate software to measure the following parameters: myelinated nerve fiber diameter (µm) and density (count/area), nerve tissue percentage, and G-ratio (myelinated axon diameter/myelinated nerve fiber diameter).
3. **Immunostaining**

1. Follow standard protocols for paraffin section staining.
2. Incubate with primary antibodies for 30 min at 25 °C.
3. Wash with phosphate-buffered saline 3 times at 25 °C.
4. Incubate with secondary antibodies labeled with horseradish-peroxidase for 30 min at 25 °C.
5. Obtain images using a light microscope.

4. **Transmission Electron Microscopy (TEM)**
   1. Prepare nerves as described in step 7.1.
   2. Section nerves at a thickness of 70 – 90 µm using an ultramicrotome.
   3. Stain sections with Reynold's lead citrate and uranyl.
   4. Examine and image by transmission electron microscopy.

Representative Results

We observed an increase in the facial skin temperature of the blocked side 1 week after the left CSGB (**Figure 8**).

At 3 months post-reconstruction, the PGA-C tube at the reconstruction area was absorbed and regeneration of the inferior alveolar nerve was observed in the reconstruction-only and reconstruction + CSGB groups (**Figure 9A, B**)[18].

SNAP was measurable in both reconstruction sides of the reconstruction + CSGB and reconstruction-only groups. The results of the electrophysiological evaluation are summarized in **Table 1**[18]. The recovery index and SCV were significantly higher in the reconstruction + CSGB than in the reconstruction-only group.

We observed myelinated nerve fibers at the central and distal segments of the regenerated IAN in the reconstruction-only and reconstruction + CSGB groups (**Figure 10A, B**)[18]. The reconstruction-only and reconstruction + CSGB groups showed smaller regenerated myelinated nerve diameters as compared to the normal control group (central segment of the right IAN in the reconstruction group, **Figure 10C**). Immature myelinated nerve fibers were also observed.

Examination of the reconstruction-only, reconstruction + CSGB groups using TEM showed regenerated myelinated nerve fibers and Schwann cells (**Figure 10D, E**). **Figure 10F** shows these results of TEM for the normal control group (central segment of the right IAN in the reconstruction group).

The presence of regenerated axons and Schwann cells was confirmed at the central and distal segments of the reconstruction-only and reconstruction + CSGB groups, by staining with anti-neurofilament (NF) and anti-S100 antibodies, respectively (**Figure 11**)[18].

Morphological evaluation results are summarized in **Table 2**[18]. The myelinated nerve fiber diameter at the center of the regenerated left IAN segment was 4.27 ± 1.5 µm in the reconstruction group and 5.11 ± 1.98 µm in the CSGB group, while at the distal segment of the regenerated left IAN the diameter was 3.47 ± 1.21 µm in the reconstruction group and 4.53 ± 1.36 µm in the CSGB group. In both cases, the diameter was significantly larger in the CSGB group, which also demonstrated a significantly higher myelinated nerve fiber density and nerve tissue percentage in both the center and the distal segment of the regenerated left IAN. The G-ratio at the center of the regenerated left IAN was 0.75 ± 0.04 in the reconstruction group and 0.68 ± 0.05 in the CSGB group, while at the distal part it was 0.74 ± 0.04 in the reconstruction group and 0.69 ± 0.04 in the CSGB group. Thus, in both cases, the G-ratio was significantly smaller in the CSGB group.

The sample sizes for the reconstruction-only and reconstruction + CSGB groups were n = 7. The statistical analyses for the myelinated nerve fiber diameter and density, G-ratio, and SCV were performed using Dunnett's test. Analysis of the recovery index was performed using an unpaired Student's *t*-test. The level of statistical significance was set at 5% ($p < 0.05$).

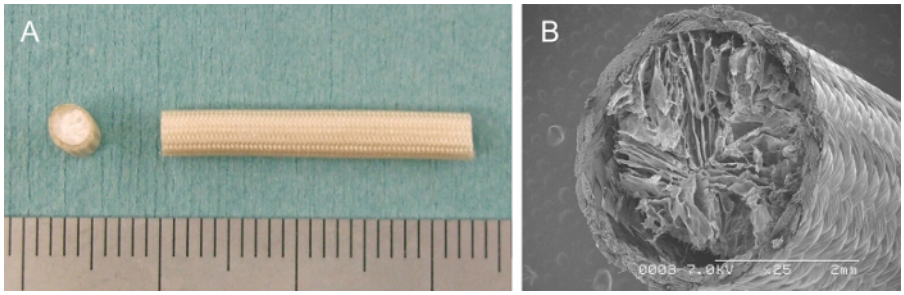

Figure 1: Polyglycolic acid tube filled with collagen sponge. A) Gross image of the tube. The final dimensions of the nerve conduit were 14 mm length, 3 mm inner diameter, and 50 µm wall thickness. **B**) Scanning electron micrograph of the tube. This figure was previously published by Shionoya *et al.*[18] and is reprinted with permission. Please click here to view a larger version of this figure.

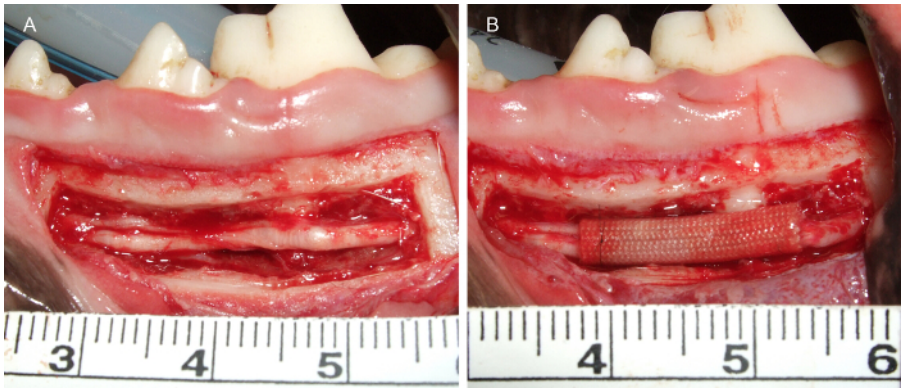

Figure 2: Left inferior alveolar nerve (IAN) pre- and post-reconstruction. A) Pre-reconstruction image of the left IAN after being exposed by removal of bone. **B**) Post-reconstruction image of the left IAN reconstructed using a polyglycolic acid-collagen tube. This figure was previously published by Shionoya *et al.*[18] and is reprinted with permission. Please click here to view a larger version of this figure.

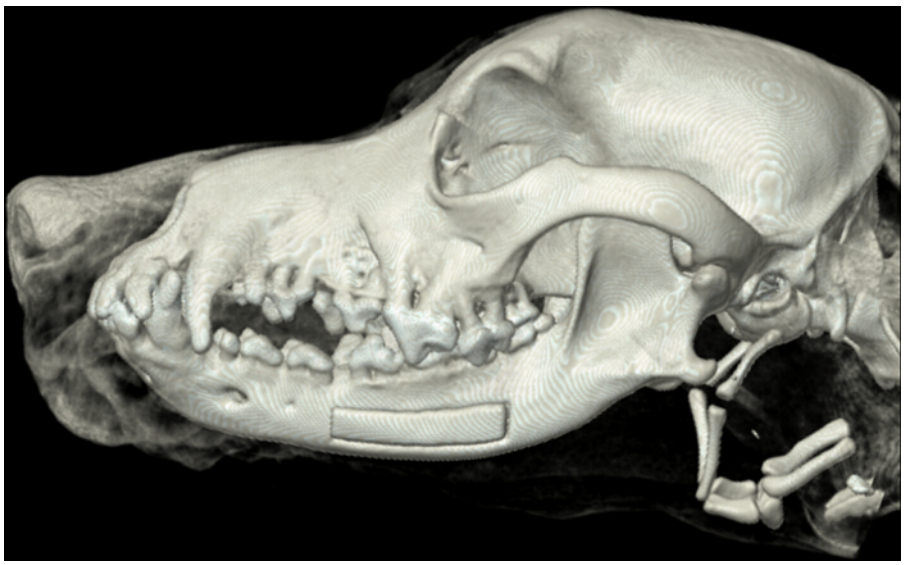

Figure 3: Computed tomography imaging of the facial bone after left inferior alveolar nerve reconstruction. The image shows that the mandibular bone plate is in the proper position. Please click here to view a larger version of this figure.

Figure 4: Pre-operative skin markings on the left side chest area prior to surgery. Photograph showing the skin markings before performing the cervical sympathetic ganglion block. The incision line is 20 cm in length. Please click here to view a larger version of this figure.

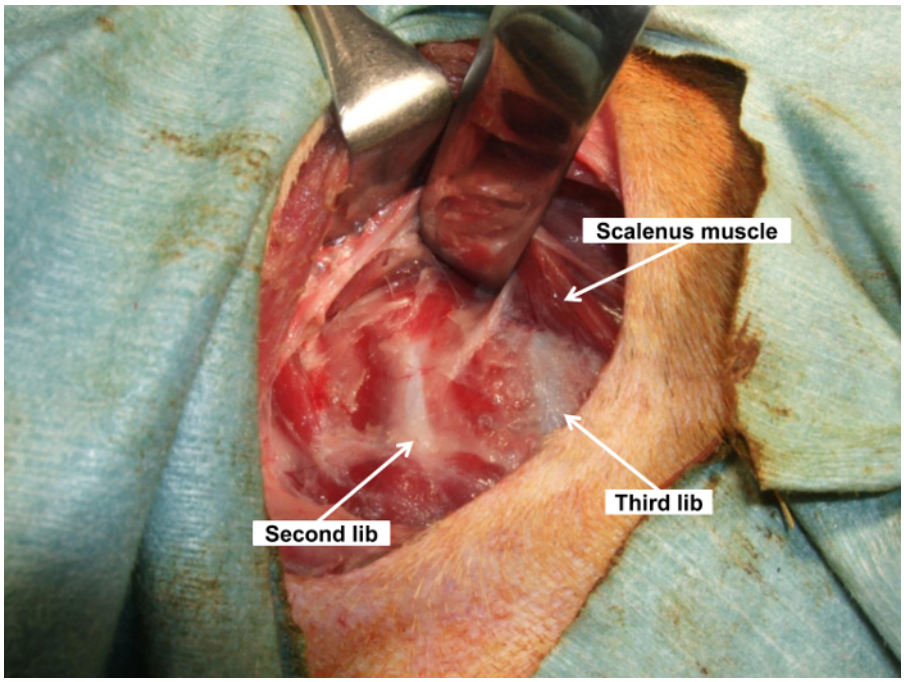

Figure 5: Operating view of the cervical sympathetic ganglion block: pre-thoracotomy. Image shows the second and third ribs after raising the serratus ventralis and scalenus muscles. Please click here to view a larger version of this figure.

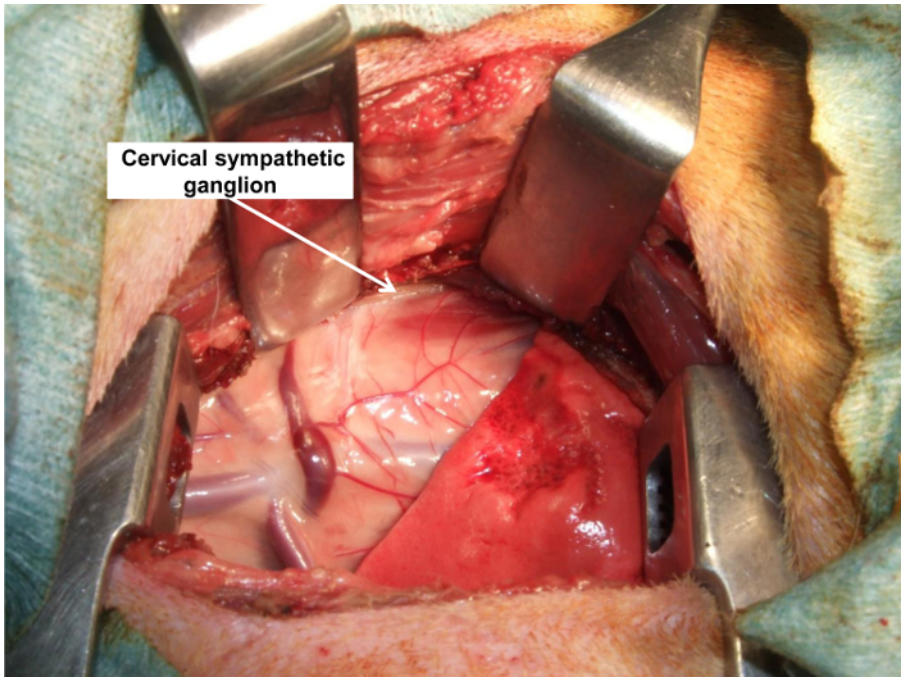

Figure 6: Operating view of the cervical sympathetic ganglion block: post-thoracotomy. Image shows the left cervical sympathetic ganglion after lateral thoracotomy at the second and third intercostal space. Please click here to view a larger version of this figure.

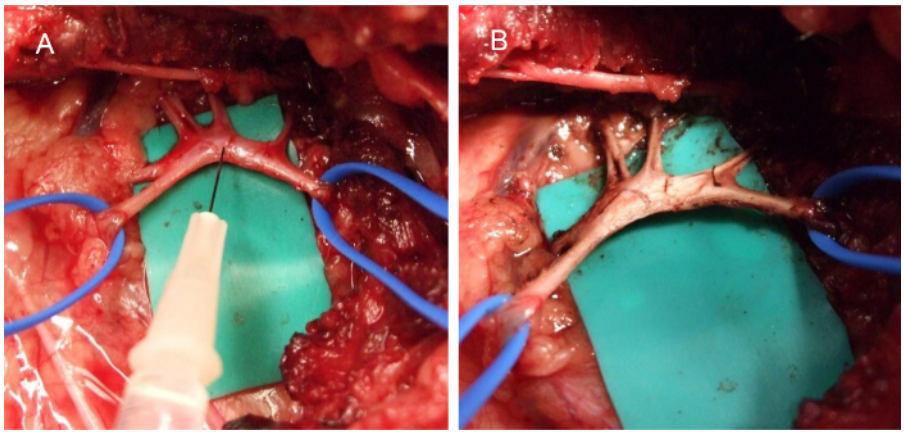

Figure 7: Cervical sympathetic ganglion pre- and post-ethanol injection using a 30 G needle. A) Pre-ethanol injection image of the left cervical sympathetic ganglion. **B**) Post-ethanol injection image of the left cervical sympathetic ganglion. Please click here to view a larger version of this figure.

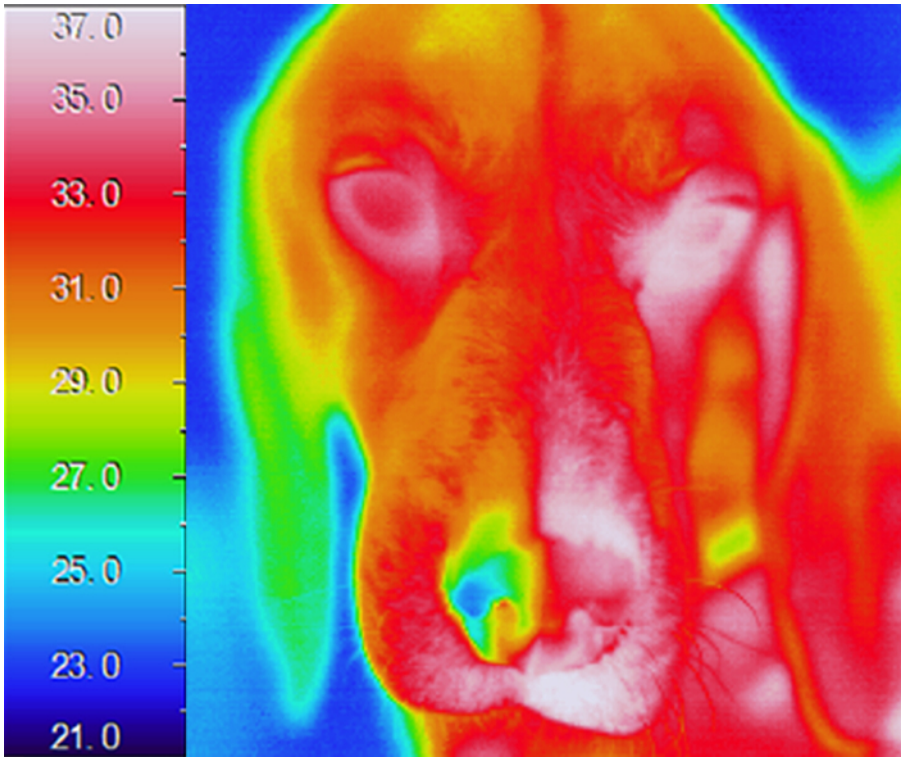

Figure 8: Thermogram after left cervical sympathetic ganglion block (CSGB). The thermogram was acquired one week after CSGB by ethanol injection. Note that the facial skin temperature on the left side is higher than on the contralateral side. The color bar indicates temperatures in °C. Please click here to view a larger version of this figure.

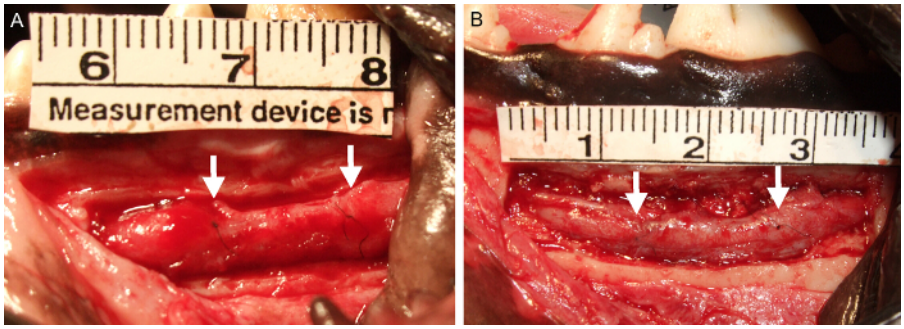

Figure 9: Regenerated inferior alveolar nerve (IAN). A) Image of the IAN in the reconstruction-only group. **B**) Image of the IAN in the reconstruction + CSGB (cervical sympathetic ganglion block) group. Nerve regeneration (region between white arrowheads) is observed in both groups. This figure was previously published by Shionoya *et al.*[18] and is reprinted with permission. Please click here to view a larger version of this figure.

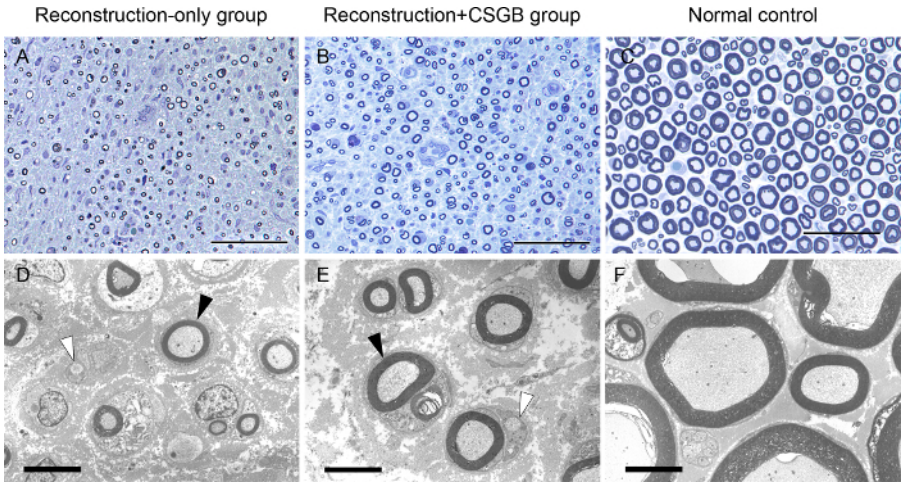

Figure 10: Toluidine blue and transmission electron microscopy analysis of the regenerated inferior alveolar nerve (IAN). A - **C**) Semi-thin transverse sections of the IAN at 3 months post-reconstruction stained with toluidine blue. Images show the distal segments of the regenerated left IAN in each group, as indicated. **D** - **F**) Transmission electron microscopy images from semi-thin sections showing myelinated and non-myelinated nerve fibers (black and white arrowheads, respectively). Scale bars represent 50 µm in (A) - (C) and 5 µm (D) - (F). Normal control: central segment of the right IAN in the reconstruction-only group. This figure was previously published by Shionoya *et al.*[18] and is reprinted with permission. Please click here to view a larger version of this figure.

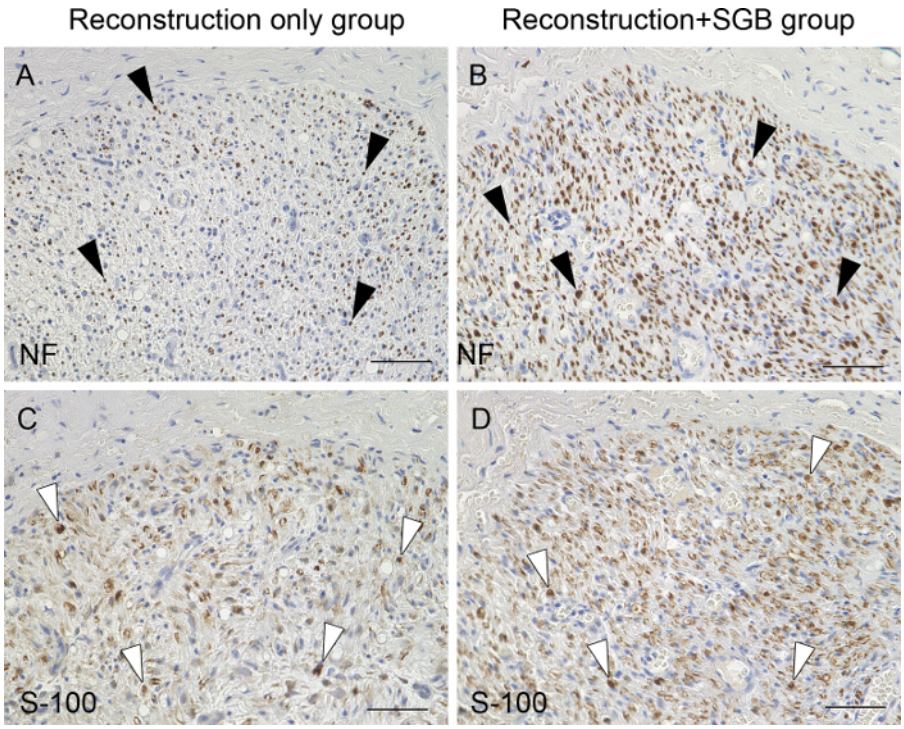

Figure 11: Immunohistochemical analysis of distal segments of the regenerated left inferior alveolar nerve (IAN). A, **B**) Sections of the regenerated IAN at 3 months post-reconstruction stained with an anti-neurofilament (NF) antibody for the reconstruction-only group (A) and reconstruction + cervical sympathetic ganglion block (CSGB; B) groups. Black arrowheads indicate regenerated axons. **C**, **D**) Sections of the regenerated IAN at 3 months post-reconstruction stained with an anti-S-100 antibody for the reconstruction-only group (C) and reconstruction + CSGB (D) groups. White arrowheads indicate Schwann cells. Scale bars, 50 µm. This figure was previously published by Shionoya *et al.*[18] and is reprinted with permission. Please click here to view a larger version of this figure.

	Sensory nerve conduction (m/s)	Recovery index
Normal control	48.5 ± 2.8	#
Reconstruction-only group	36.8 ± 2.9*	0.22 ± 0.04
Reconstruction+CSGB group	42.0 ± 2.4*#	0.35 ± 0.06#

Table 1: Electrophysiological findings in theinferior alveolar nerve (IAN) at 3 months after surgery. Data are presented as mean ± standard deviation (n = 7). Comparisons were made using an unpaired Student's *t*-test. IAN, inferior alveolar nerve; CSGB, cervical sympathetic ganglion block. *, $p < 0.05$ in comparison with the normal control group; #, $p < 0.05$ in comparison with the reconstruction-only group. Normal control: central segment of the right IAN in the reconstruction-only group; Recovery index: ratio of the peak amplitude of the left IAN of the reconstruction-only or reconstruction + CSGB group to the peak amplitude of the normal control. This table was previously published by Shionoya *et al.*[18] and is reprinted with permission.

		Myelinated nerve fiber diameter (μm)	Myelinated nerve fiber density (count/100 μm^2)	Proportion of nerve tissue (%)	G ratio
Normal control	Center	8.83 ± 3.11	103 ± 8	41.3 ± 3.9	0.62 ± 0.03
Reconstruction-only group	Center	4.27 ± 1.5*	126 ± 20*	11.6 ± 2.1*	0.75 ± 0.04*
	Distal	3.47 ± 1.21*	109 ± 17*	7.3 ± 2.0*	0.74 ± 0.04*
Reconstruction+CSGB group	Center	5.11 ± 1.98*#	140 ± 22*#	15.9 ± 3.0*#	0.68 ± 0.05*#
	Distal	4.53 ± 1.36*$	123 ± 15*$	12.5 ± 2.1*$	0.69 ± 0.04*$

Table 2: Morphological findings in the inferior alveolar nerve (IAN) at 3 months after surgery. Data are presented as mean ± standard deviation (n = 7). Comparisons were made using Dunnett's test. IAN, inferior alveolar nerve; CSGB, cervical sympathetic ganglion block. *, $p < 0.05$ in comparison with the normal control group; #, $p < 0.05$ in comparison with the central segment of the left IAN in the reconstruction-only group; $, $p < 0.05$ in comparison with the distal end of the left IAN in the reconstruction-only group. Normal control: central segment of the right IAN in the reconstruction-only group; G ratio is the ratio of the myelinated axon diameter to the total myelinated fiber diameter. This table was previously published by Shionoya *et al.*[18] and is reprinted with permission.

Discussion

We present an efficient method for IAN regeneration by using a bioabsorbable nerve tube in combination with ethanol-induced CSGB. For this study we used dogs, since other animal models, like mice, rats, and rabbits, have a short life expectancy and small body size, and hence cannot be used to perform the precise surgical procedures. As the IAN is located within the mandibular canal surrounded by bone, a surgical technique is necessary to avoid nerve and blood vessel damage when performing nerve reconstruction. An important technical tip for the procedure is to carefully remove the mandibular bone plate in order to minimize the risk of nerve and vessel injury. Traditional burs and micro saws cannot distinguish between hard and soft tissue[21]. Additionally, these tools tend to slip causing damaging the adjacent tissue, especially the IAN, by accidental contact[22]. We therefore used piezoelectric surgical tools for the bone processing steps. This is a new and innovative bone surgery technique that uses ultrasonic microvibrations of specialized scalpels. Therefore, soft tissue are not damaged even upon accidental contact with the cutting tips[23,24]. Microvibrations of 60 - 200 μm/s at 24 - 29 kHz are optimal for cutting elastic mineralized tissue while sparing elastic soft tissue; this is not possible at frequencies above 50 kHz[25]. Moreover, rotational burs or oscillating saws require a force to counteract the rotation or vibration of the instrument. Compared to these instruments, piezoelectric surgical tools do not need application of extra force and so safe and accurate bone processing is possible[26]. This is especially important in the hands of a novel user.

Another important aspect in our method is that the bone plate was not fixed using metallic plates but was placed in its original position in the mandible after the placement of the PGA-C tube. The reason for this was to avoid the risk of exposure of the plate to oral mucosal necrosis, which arises when using metallic plates for fixation. However, in some cases the bone plate deviated from the original site. Therefore, it is crucial to perform a CT scan of the facial bone to confirm that the mandibular bone plate is in the proper position after surgery. When using a metallic plate for fixation, tight suturing should be avoided as it may cause oral mucosal necrosis due to blood flow disturbances.

CSGB is an effective treatment for peripheral vascular diseases and pain syndromes of the face and neck[13,14,15]. However, the mechanisms underlying its therapeutic effects remain unclear. One reason for the lack of research on the therapeutic effects of CSGB is the difficulty in obtaining a consistent and uniform sympatholytic effect. For example, the spread of sympathetic blockade after percutaneous CSGB is not uniform[27,28]. Mullenheim *et al.*[29] implanted dogs with a polyethylene catheter, after thoracotomy, under the fascia and alongside the upper sympathetic chain, and performed CSGB by injecting lidocaine via the catheter. Although this approach can spread sympathetic blockade at the targeted areas, it carries risks of catheter occlusion or dislocation, as well as infection, especially in long-term experiments. In our canine model of CSGB, the direct injection of 99.5% ethanol produced long-term increases in blood flow to the ipsilateral orofacial region. In our approach, block injection was administered under direct visualization, so CSGB could be performed with precision. Therefore, our approach reduces the risk of uneven spread of the sympatholytic effect and of the sympathetic blockade. This is considered to be advantageous especially in long-term experiments. Moreover, we used thermography to confirm the success of CSGB, since facial skin temperature increases on the block side upon successful CSGB. In this case, thermography is useful, because it is simple and noninvasive. Importantly, the nasal and not the facial skin temperature should be measured, since it is not affected by the dog's hair. Our model could contribute to further research on the therapeutic effects of CSGB. In our previous study, blood flow in the orofacial area increased for 6-11 weeks after cervical sympathetic ganglionectomy. Researchers can choose this alternative method[30] if desired.

The limitation of this study is that ethanol-induced CSGB poses the risk of developing permanent Horner's syndrome (ptosis and miosis)[31]. Other methods, including radiofrequency ablation, phenol, and sympathetic ganglionectomy have been used for performing sympathectomies; however, specifically for sympathectomy of the cervical sympathetic ganglion, only radiofrequency ablation has been employed in clinical practice[32,33,34,35]. Therefore, radiofrequency ablation and local anesthetics can be considered as an alternative method to ethanol-induced CSGB. Future studies would be necessary to validate how nerve regeneration mediated by a bioabsorbable nerve tube can be enhanced by CSGB with a local anesthetic or radiofrequency ablation.

Disclosures

The authors have nothing to disclose.

Acknowledgements

This work was supported by the Department of Bioartificial Organs in Kyoto University Institute for Frontier Medical Science. We would like to thank the veterinary staff of the Institute for Frontier Medical Science.

References

1. Al-Sabbagh, M., Okeson, J.P., Bertoli, E., Medynski, D.C., Khalaf, M.W. Persistent pain and neurosensory disturbance after dental implant surgery: prevention and treatment. *Dental Clinics of North America.* **59** (1), 143-156 (2015).
2. Chaushu, G., Taicher, S., Halamish-Shani, T., Givol, N. Medicolegal aspects of altered sensation following implant placement in the mandible. *International Journal of Oral and Maxillofacial Implants.* **17** (3), 413-415 (2002).
3. Robinson, P.P., Loescher, A.R., Yates, J.M., Smith, K.G. Current management of damage to the inferior alveolar and lingual nerves as a result of removal of third molars. *British Journal of Oral and Maxillofacial Surgery.* **42** (4), 285-292 (2004).
4. Gregg, J.M. Studies of traumatic neuralgia in the maxillofacial region: symptom complexes and response to microsurgery. *Journal of Oral and Maxillofacial Surgery.* **48** (2), 135-140 (1990).
5. Pogre, M.A. The results of microneurosurgery of the inferior alveolar and lingual nerve. *Journal* of *Oral and Maxillofacial Sureryg.* **60** (5), 485-489 (2002).
6. Strauss, E.R, Ziccardi, V.B, Janal, M.N. Outcome assessment of inferior alveolar nerve microsurgery: a retrospective review. *Journal of Oral and Maxillofacial Surgery.* **64** (12), 1767-1770 (2006).
7. Nakamura, T., *et al.* Experimental study on the regeneration of peripheral nerve gaps through a polyglycolic acid-collagen (PGA-collagen) tube. *Brain Research.* **1027** (1-2), 18-29 (2004).
8. Yoshitani, M., *et al.* Experimental repair of phrenic nerve using a polyglycolic acid and collagen tube. *Journal of Thoracic and Cardiovascular Surgery.* **133** (3), 726-732 (2007).
9. Seo, K., *et al.* One-year outcome of damaged lingual nerve repair using a PGA-collagen tube: a case report. *Journal of Oral and Maxillofacial Surgery.* **66** (7), 1481-1484 (2008).
10. Seo, K., *et al.* Protracted delay in taste sensation recovery after surgical lingual nerve repair: a case report. *Journal of Medical Case Reports.* **7**, 77 (2013).
11. Seo, K., Terumitsu, M., Inada, Y., Nakamura, T., Shigeno, K., Tanaka, Y. Prognosis after surgical treatment of trigeminal neuropathy with a PGA-c tube: report of 10 Cases. *Pain Medicine.* **17** (12), 2360-2368 (2016).
12. Okuda, Y., Kitajima, T. Comparison of stellate ganglion block with intravascular infusion of prostaglandin e1 on brachial artery blood flow in dogs. *Anesthesia and Analgesia.* **84** (6), 1329-1332 (1997).
13. Kohjitani, A., Miyawaki, T., Kasuya, K., Shimada, M. Sympathetic activity-mediated neuropathic facial pain following simple tooth extraction: a case report. *Cranio.* **20** (2), 135-138 (2002).
14. Melis, M., Zawawi, K., al-Badawi, E., Lobo Lobo, S., Mehta, N. Complex regional pain syndrome in the head and neck: a review of the literature. *Journal of Orofacial Pain.* **16** (2), 93-104 (2002).
15. Salvaggio, I., Adducci, E., Dell'Aquila, L., Rinaldi, S., Marini, M., Zappia, L., Mascaro, A. Facial pain: a possible therapy with stellate ganglion block. *Pain Medicine.* **9** (7), 958-962 (2008).
16. Atsumi, M., Sunada, K. The effect of superior cervical ganglion resection on peripheral facial palsy in rats. *Journal of Anesthesia.* **30** (4), 677-683 (2016).
17. Hanamatsu, N., Yamashiro, M., Sumitomo, M., Furuya, H. Effectiveness of cervical sympathetic ganglia block on regeneration of the trigeminal nerve following transection in rats. *Regional Anesthesia and Pain Medicine.* **27** (3), 268-276 (2002).
18. Shionoya, Y., Sunada, K., Shigeno, K., Nakada, A., Honda, M., Nakamuram T. Can nerve regeneration on an artificial nerve conduit be enhanced by ethanol-induced cervical sympathetic ganglion block? *PLoS One.* **12** (12), e0189297 (2017).
19. Suzuki, Y., Tanihara, M., Ohnishi, K., Suzuki, K., Endo, K., Nishimura, Y. Cat peripheral nerve regeneration across 50 mm gap repaired with a novel nerve guide composed of freeze-dried alginate gel. *Neuroscience Letters.* **259** (2), 75-78 (1999).
20. Ichihara, S., *et al.* Development of new nerve guide tube for repair of long nerve defects. *Tissue Engineering, Part C, Methods.* **15** (3), 387-402 (2009).
21. Grenga, V., Bovi, M. Piezoelectric surgery for exposure of palatally impacted canines. *Journal of Clinical Orthodontics.* **38**, 446-448 (2004).
22. Degerliyurt, K., Akar, V., Denizci, S., Yucel, E. Bone lid technique with piezosurgery to preserve inferior alveolar nerve. *Oral Surgery, Oral Medicine, Oral Pathology, Oral Radiology, and Endodontology.* **108** (6), e1-5 (2009).
23. Kotrikova, B., *et al.* Piezosurgery-a new safe technique in cranial osteoplasty? *International Journal of Oral and Maxillofacial Surgery.* **35** (5), 461-465 (2006).
24. Vercellotti, T. Piezoelectric surgery in implantology: a case report-a new piezoelectric ridge expansion technique. *International Journal of Periodontics and Restorative Dentistry.* **20** (4), 358-365 (2000).
25. Stübinger, S., Kuttenberger, J., Filippi, A., Sader, R., Zeilhofer, H.F. Intraoral piezosurgery: Preliminary results of a new technique. *Journal of Oral and Maxillofacial Surgery.* **63** (9), 1283-1287 (2005).

26. Eggers, G., Klein, J., Blank, J., Hassfeld, S. Piezosurgery: an ultrasound device for cutting bone and its use and limitations in maxillofacial surgery. *British Journal of Oral and Maxillofacial Surgery.* **42** (5), 451-453 (2004).
27. Hardy, P.A., Wells, J.C. Extent of sympathetic blockade after stellate ganglion block with bupivacaine. *Pain.* **36** (2), 193-196 (1989).
28. Hogan, Q.H., Erickson, S.J., Haddox, J.D., Abram, S.E. The spread of solutions during stellate ganglion block. *Regional Anesthesia.* **17** (2), 78-83 (1992).
29. Mullenheim, J., *et al.* Left stellate ganglion block has only small effects on left ventricular function in awake dogs before and after induction of heart failure. *Anesthesia and Analgesia.* **91** (4), 787-792 (2000).
30. Tsujimoto, G., Sunada, K., Nakamura, T. Effect of cervical sympathetic ganglionectomy on facial nerve reconstruction using polyglycolic acid-collagen tubes. *Brain Research.* **1669**, 79-88 (2017).
31. Ghai, A., Kaushik, T., Kumar, R., Wadhera, S. Chemical ablation of stellate ganglion for head and neck cancer pain. *Acta Anaesthesiologica Belgica.* **67** (1), 6-8 (2016).
32. Forouzanfar, T., van Kleef, M., Weber, W.E. Radiofrequency lesions of the stellate ganglion in chronic pain syndromes: retrospective analysis of clinical efficacy in 86 patients. *Clinical Journal of Pain.* **16** (2), 164-168 (2000).
33. Ohno, K., Oshita, S. Transdiscal lumbar sympathetic block: a new technique for a chemical sympathectomy. *Anesthesia and Analgesia.* **85** (6), 1312-1316 (1997).
34. Slappendel, R., Thijssen, H.O., Crul, B.J., Merx, J.L. The stellate ganglion in magnetic resonance imaging: a quantification of the anatomic variability. *Anesthesiology.* **83** (2), 424-426 (1995).
35. Wang, Y.C., Wei, S.H., Sun, M.H., Lin, C.W. A new mode of percutaneous upper thoracic phenol sympathicolysis: report of 50 cases. *Neurosurgery.* **49** (3), 628-634 (2001).

